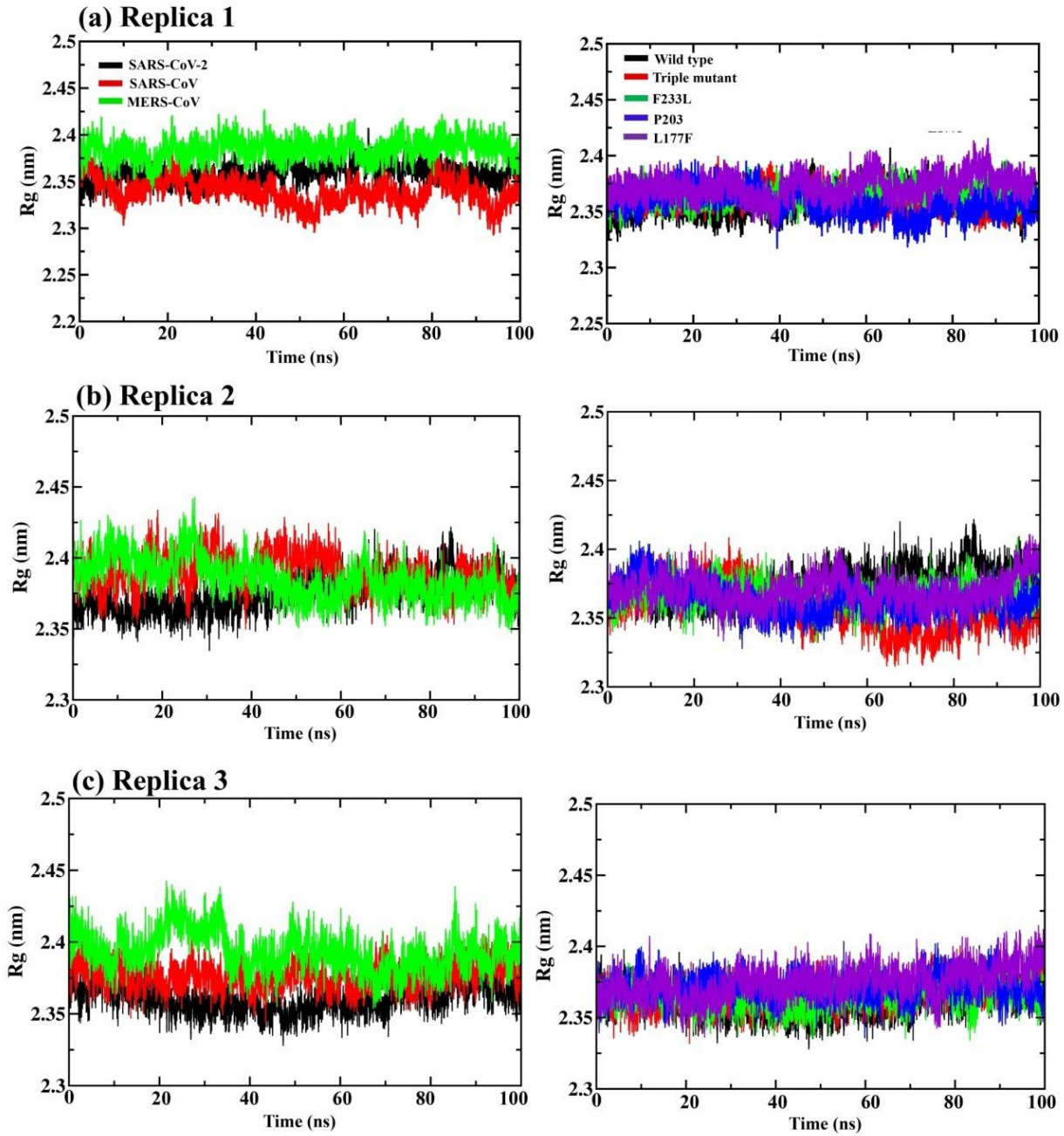
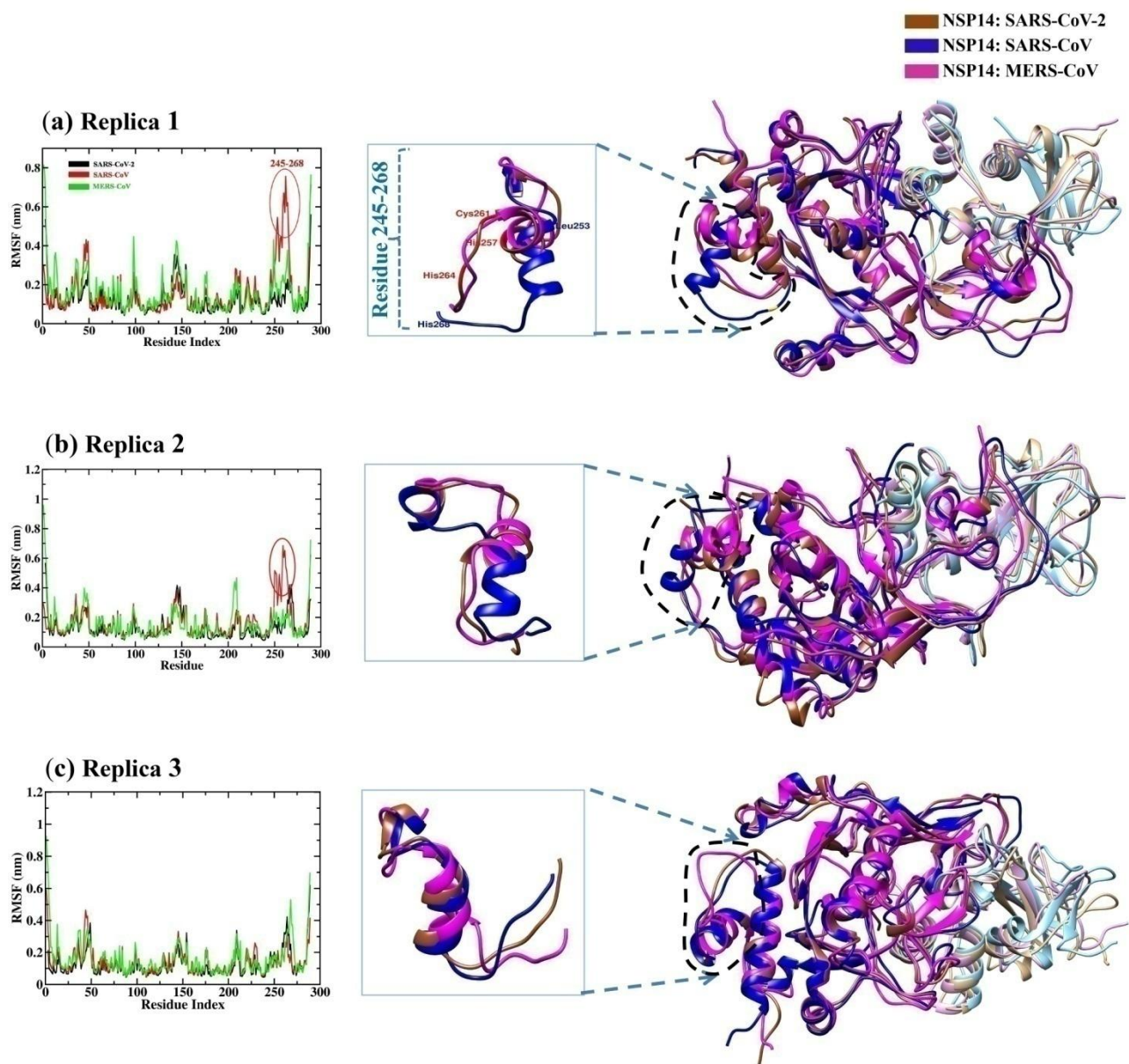


**Figure S3.** Representation of hydrophobicity map of average structure (from last 20 ns) SARS-CoV-2 (a), SARS-CoV (b) and (c) MERS-CoV NSP14-NSP10 PPI complex in three different forms. Yellow colour depiction is for NSP10, Brown colour is NSP14. The nonpolar (orange), polar (blue) and neutral regions are depicted for the NSP14.



**Figure S4.** Radius of gyration (Rg) graphs (a) – (c) of NSP14-NSP10 complexes of SARS-CoV-2, SARS-CoV, MERS-CoV (left side) and SARS-CoV-2 NSP14<sup>mutant</sup> complexes (right side) along the three sets of 100 ns MD simulation. Triple mutant (in red, in the left plots) is the combination of the three (F233L, P203, L177F) mutations.



**Figure S5.** Superimposed average structures (extracted from the last 20 ns MD trajectories of three sets of MD simulation) of SARS-CoV-2 NSP14-NSP10 complex with SARS-CoV and MERS-CoV (a)-(c). On the left side is the NSP14 RMSF plot depicts the C-terminal fluctuating residues encircled in red (from residue 245-268) in replica 1 (a) and 2 (b). The middle square box represents the corresponding fluctuating residue (245-268).

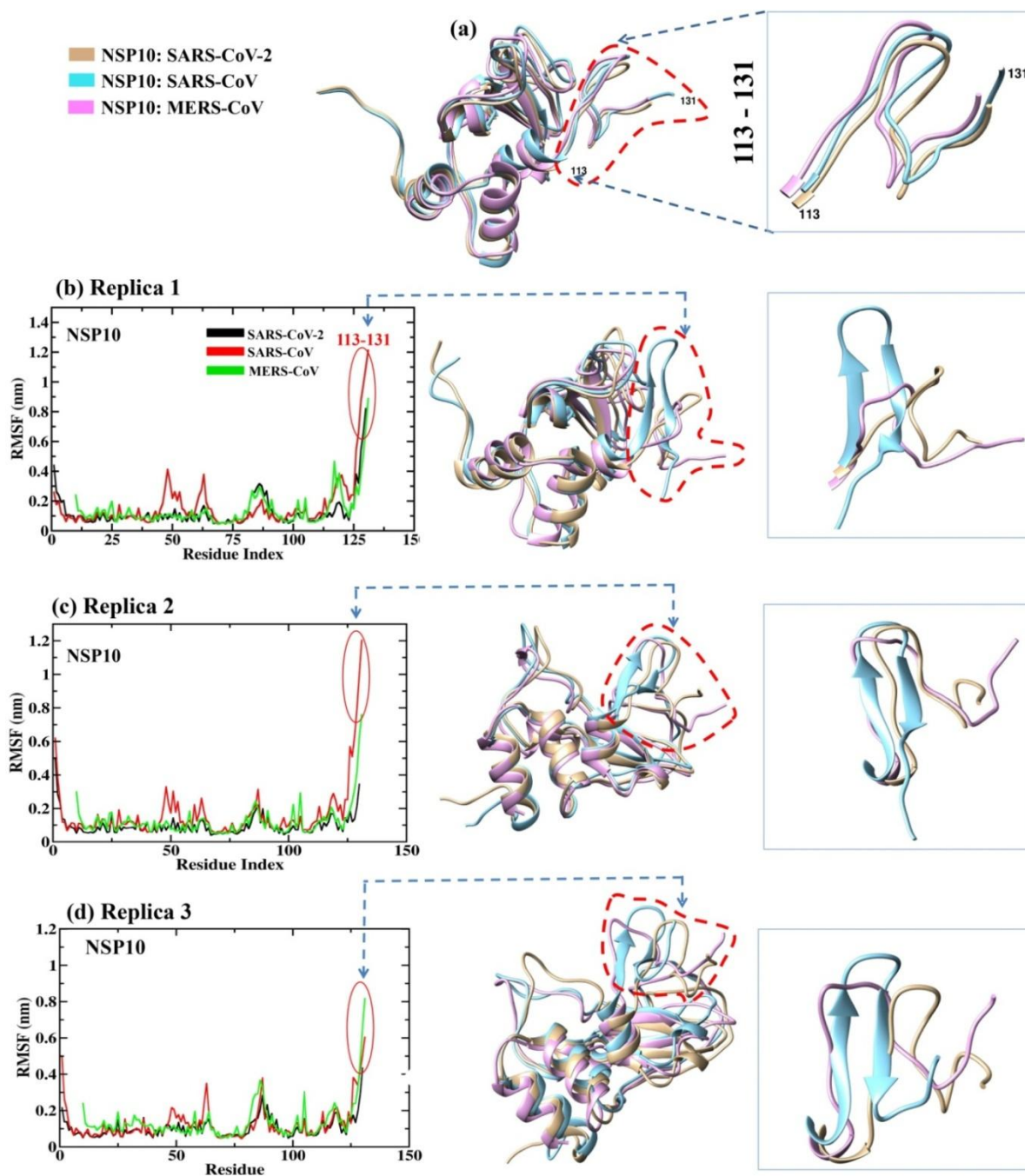


**Figure S6** Superimposed average structures(from last 20 ns) of (a) NSP10 SARS-CoV-2(light brown), SARS-CoV (cyan) and MERS-CoV (pink) from the three (b)-(d) sets of MD simulation. Left side represents the RMSF of NSP10 from the three sets of MD simulation (b)-(d). In the middle, superimposed NSP10 3D structure of the three viruses is depicted. On the right side in a square box fluctuating N-terminal region has been focused ranging from 113-131, shows a conformational change from coil to beta strand in case of SARS-CoV (cyan) in all the three sets (b)-(d) of MD simulations.

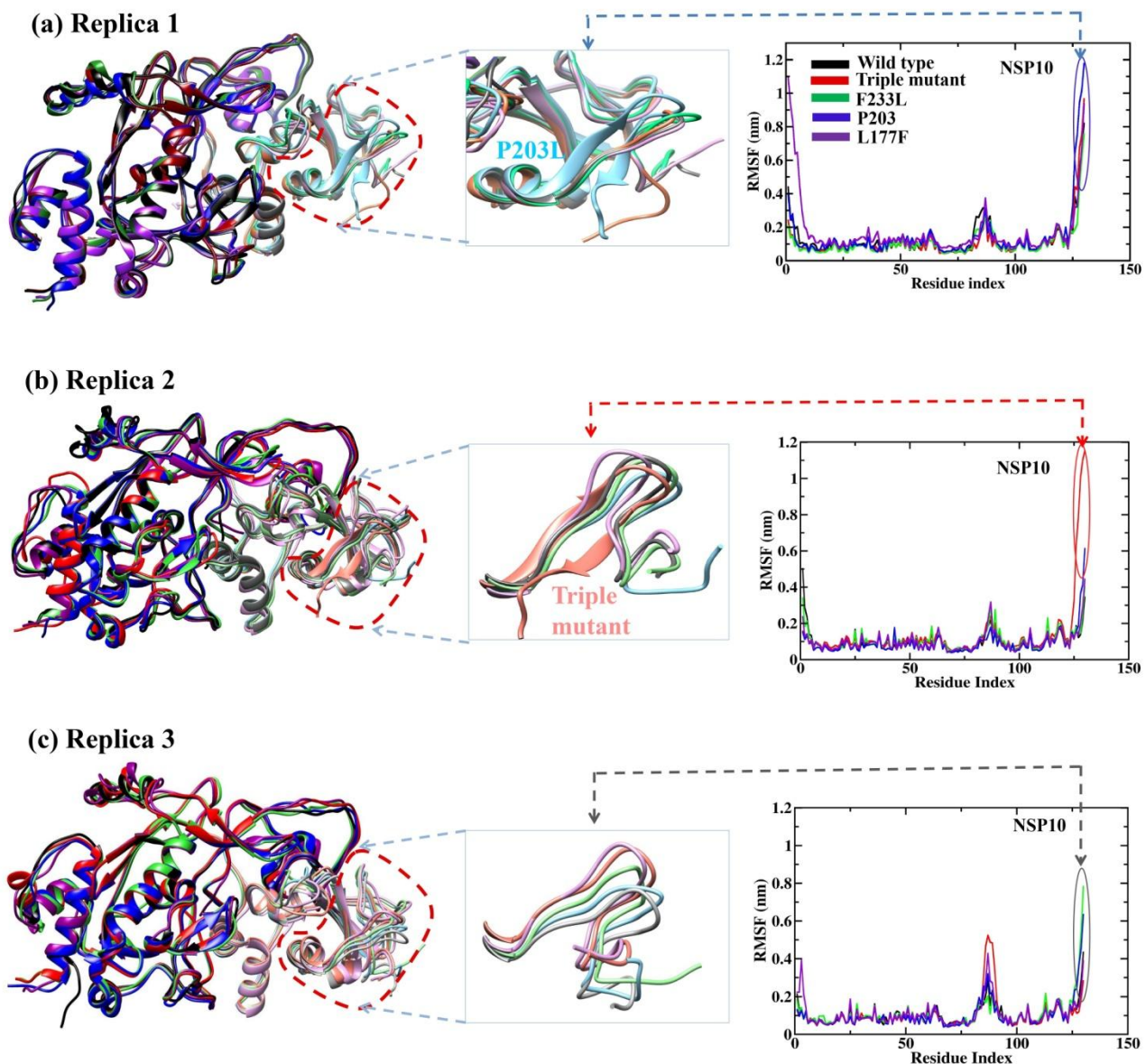


**Figure S7.** (a) – (c) On the left side, representation of superimposed SARS-CoV-2 mutant average structures (from last 20 ns) of NSP14-NSP10 from all the three sets of MD simulations. In a square box in the middle, represented the C terminal fluctuation ranging from residue 113-131 in the NSP10 when it is in complex with mutated NSP14. (a) In case of replica 1, NSP10 with NSP14 (P203L) mutant, shows a conformational change from coil to beta strand. (b) In replica 2, NSP10 with NSP14 (Triple) mutant, shows a conformational change from coil to beta strand. (c) In replica 3, in the right side RMSF plot, does not show much fluctuation as compared to replica 1 and 2, therefore there are no conformational changes observed at position 113-131 (in the middle figure in a square box of replica 3).

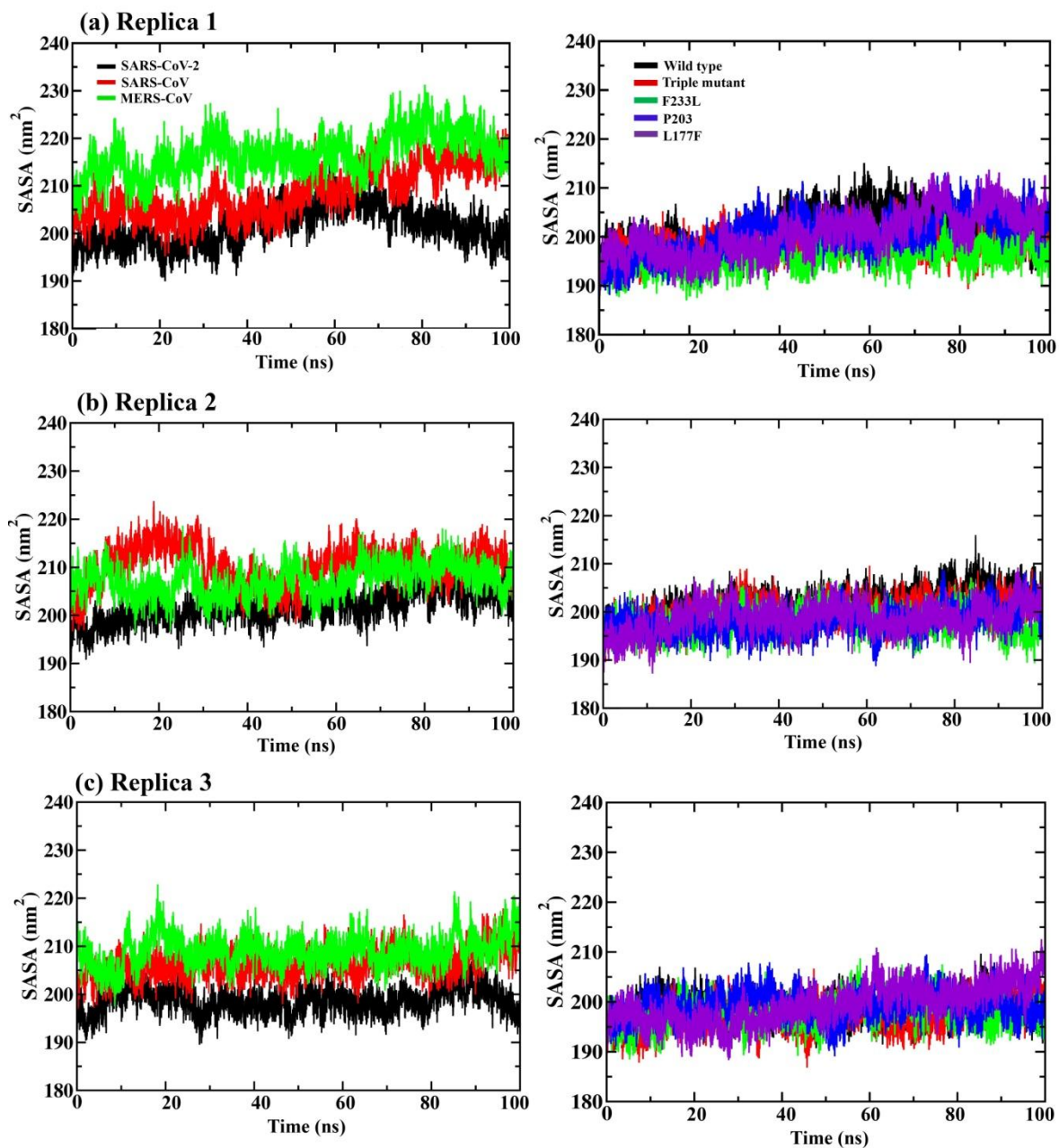


**Figure S8.** Solvent Accessible Surface Area (SASA) graphs of (a)-(c) SARS-CoV-2, SARS-CoV, MERS-CoV (left side) and SARS-CoV-2 NSP14<sup>mutant</sup> complexes (right side) along the three sets of 100 ns MD simulation.



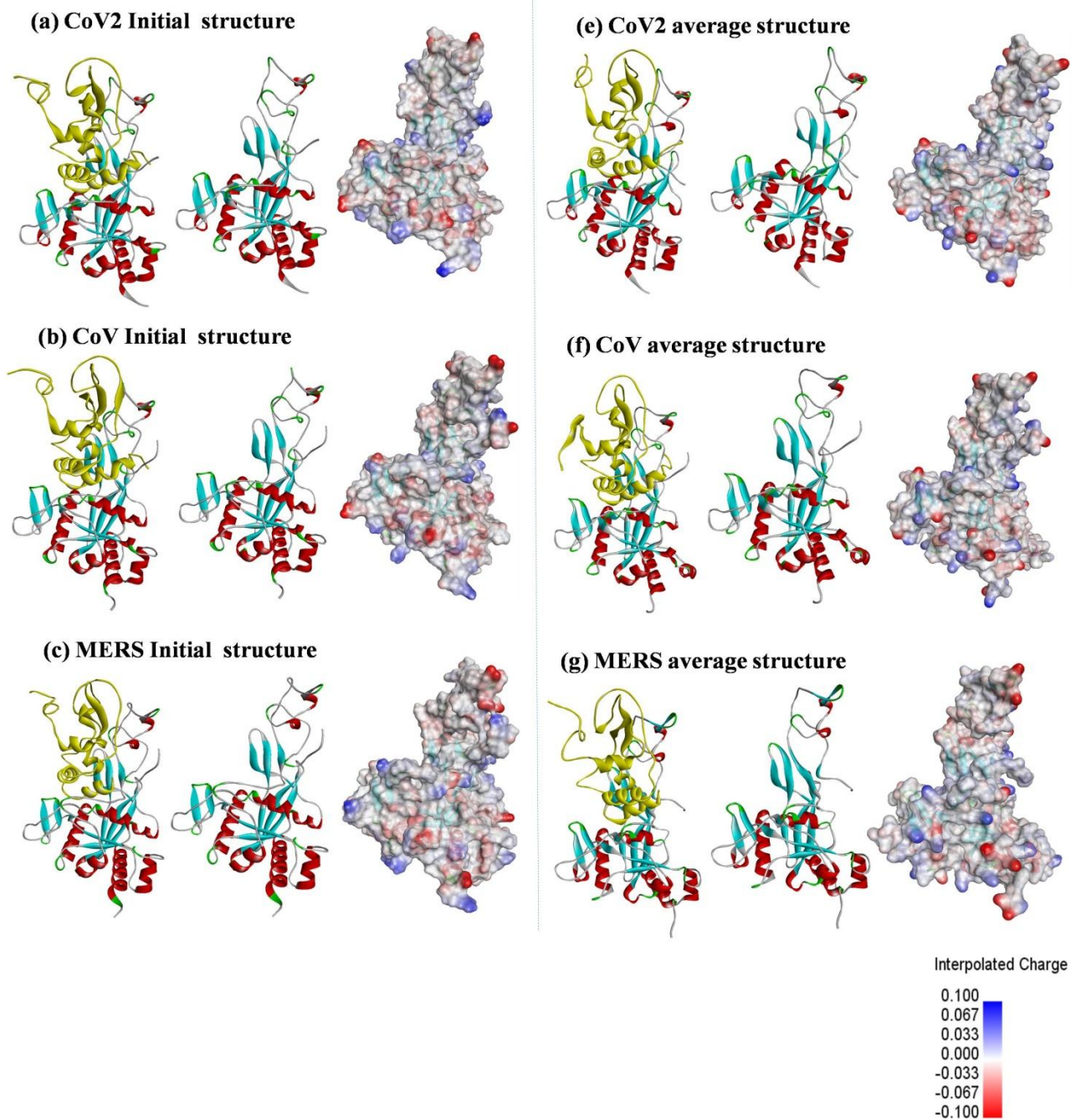


**Figure S9.** Comparison of the electrostatic surface and charge distribution of NSP14 initial (a)-(c) and average structure (extracted from last 20 ns) (e)-(g) of SARS-CoV-2, SARS-CoV and MERS-CoV. Three views are shown for each PPI complexes. NSP10 secondary structure is depicted in yellow and NSP14 presented in multicolor ribbon and electrostatic charge distribution depicting interface region of NSP14 is shown with positive (blue), negative (red) surface.

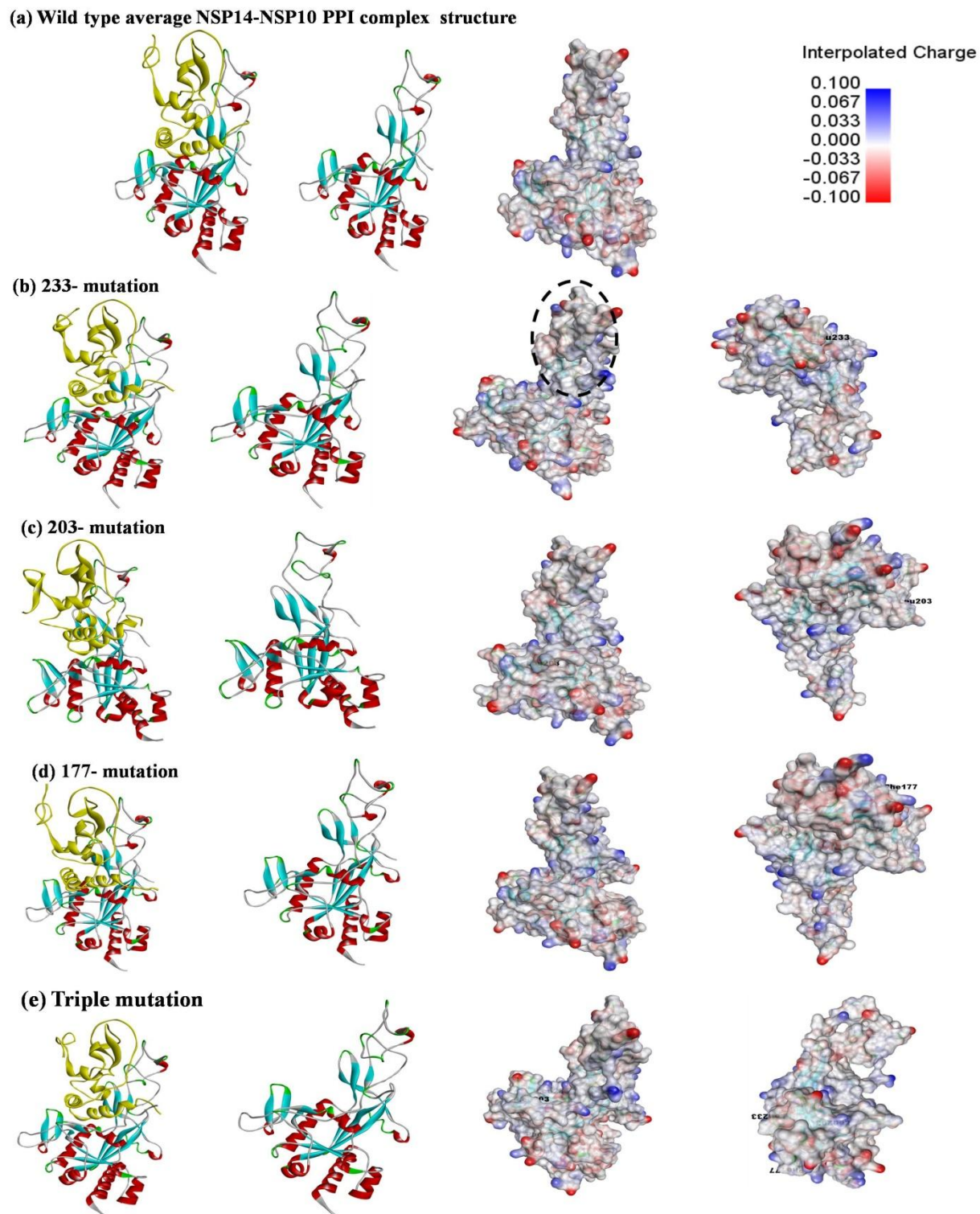


**Figure S10.** Electrostatic surfaces and charge distribution of the NSP14:comparison of the electrostatic surface of the average structure (extracted from last 20 ns) of wild type NSP14 (a) in comparison with different mutant structures (b)-(e). Three views are shown for each PPI complexes. The encircled area (b) in NSP14 (presented in multicolor as ribbon) is the binding interface region for NSP10 (NSP10 is depicted in yellow ribbon, extreme left side).

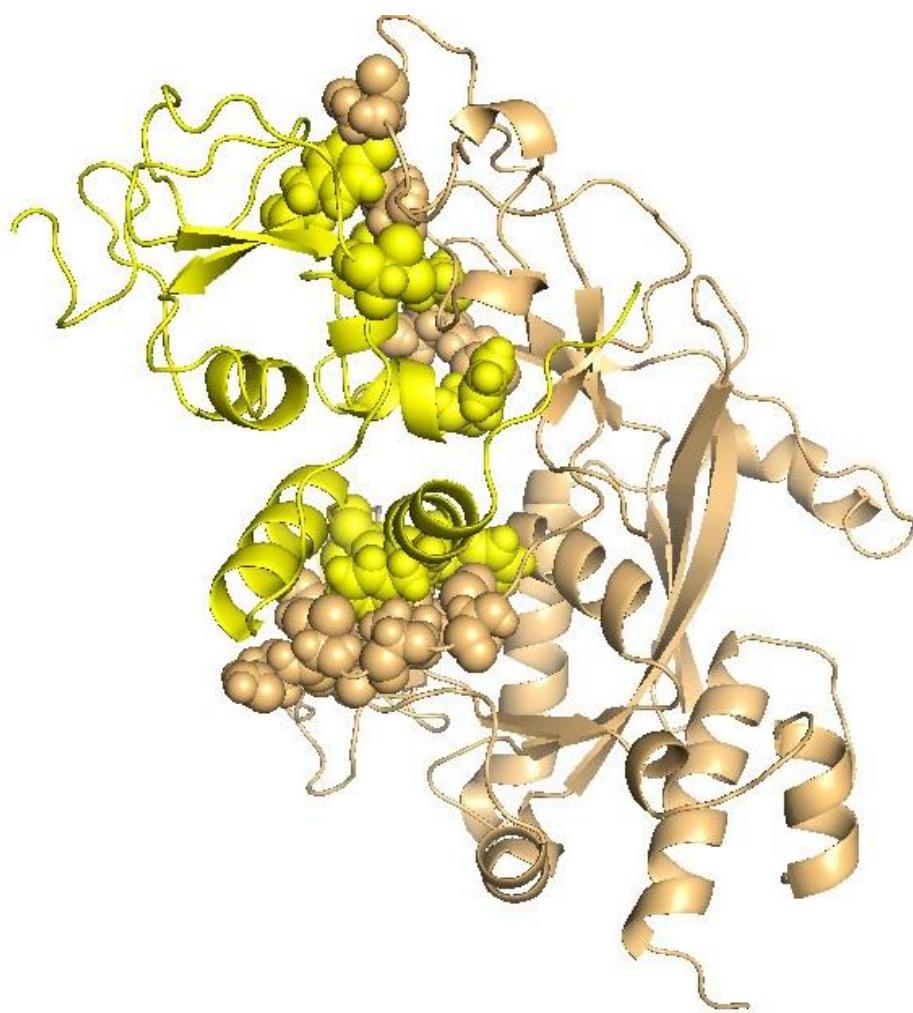


**Figure S11.** Cartoon view of the NSP14-NSP10 complex of SARS-CoV-2, common interacting interface hotspot residues among the three viruses (SARS-CoV-2, SARS-CoV and MERS-Co) represented in spheres. The NSP14 is represented in brown, NSP10 in yellow. Hotspot residues are represented in brown spheres (in NSP14), yellow spheres (in NSP10). The represented structure is the average conformer extracted from last 20 ns MD trajectory.

**Table S1.** PBC cubic box information for SARS-CoV-2, SARS-CoV and MERS-CoV

PBC Box information	SARS-CoV-2			SARS-CoV			MERS-CoV		
	x	y	z	x	y	z	x	y	z
Box vectors/size (nm)	7.80	5.94	6.63	8.16	5.76	5.65	7.83	6.28	6.02
Box volume (nm <sup>3</sup> )	279.28			265.63			292.33		

**Table S2.** Comparison of interface statistics of the initial NSP14-NSP10 complexes (before MD) of SARS-CoV-2, SARS-CoV and MERS-CoV with the average complex structures extracted from last 20 ns from 100 ns MD trajectory of replica 1. For each complex, interface statistics obtained from PDBsum server.

Human CoVs	Time	Protein chains PPI complexes	#Interface residues	Interface area (Å <sup>2</sup> )	#Salt bridges	# H-bonds	# non-bonded contacts
SARS-CoV-2	Initial structure	NSP14 (A)	50	2135	1	22	313
		NSP10 (B)	45	2320			
	Average structure from last 20 ns	<b>NSP14 (A)</b>	<b>36</b>	<b>1847</b>	<b>1</b>	<b>12</b>	<b>171</b>
		<b>NSP10(B)</b>	<b>35</b>	<b>1994</b>			
SARS-CoV-2 <sup>F233L</sup>	Average structure from last 20 ns	NSP14 (A)	38	1983	1	17	165
		NSP10(B)	37	2042			
SARS-CoV-2 <sup>P203L</sup>	Average structure from last 20 ns	NSP14 (A)	36	1898	1	13	162
		NSP10(B)	35	1970			
SARS-CoV-2 <sup>L177F</sup>	Average structure from last 20 ns	NSP14 (A)	32	1585	1	10	125
		NSP10(B)	29	1683			
SARS-CoV-2 <sup>Triple-mutant</sup>	Average structure from last 20 ns	NSP14 (A)	39	2036	1	17	178
			NSP10(B)	40			
SARS-CoV	Initial structure	NSP14 (A)	42	2004	1	14	217
		NSP10 (B)	39	2182			
	Average structure from last 20 ns	<b>NSP14 (A)</b>	<b>39</b>	<b>2062</b>	<b>1</b>	<b>17</b>	<b>175</b>
		<b>NSP10 (B)</b>	<b>39</b>	<b>2026</b>			
MERS-CoV	Initial structure	NSP14 (A)	42	1797	2	8	575
		NSP10 (B)	39	1989			
	Average structure from last 20 ns	<b>NSP14 (A)</b>	<b>30</b>	<b>1594</b>	<b>1</b>	<b>10</b>	<b>125</b>
		<b>NSP10 (B)</b>	<b>26</b>	<b>1630</b>			

**Table S3.** Comparison of interface statistics of the initial NSP14-NSP10 complexes (before MD) of SARS-CoV-2, SARS-CoV and MERS-CoV with the average complex structures extracted from last 20 ns from 100 ns MD trajectory of replica 2. For each complex, interface statistics obtained from PDBsum server.

Human CoVs	Time	Protein chains PPI complexes	#Interface residues	Interface area (Å <sup>2</sup> )	#Salt bridges	# H-bonds	# non-bonded contacts
SARS-CoV-2	Initial structure	NSP14 (A)	50	2135	1	22	313
		NSP10 (B)	45	2320			
	Average structure from last 20 ns	<b>NSP14 (A)</b>	<b>31</b>	<b>1907</b>	<b>-</b>	<b>19</b>	<b>162</b>
		<b>NSP10(B)</b>	<b>32</b>	<b>1994</b>			
SARS-CoV-2 <sup>F233L</sup>		NSP14 (A)	35	1942	-	14	165
SARS-CoV-2 <sup>P203L</sup>	Average structure from last 20 ns	NSP14 (A)	42	2016	1	15	186
		NSP10(B)	35	2126			
SARS-CoV-2 <sup>L177F</sup>		NSP14 (A)	38	2020	1	14	181
		NSP10(B)	37	2113			
SARS-CoV-2 <sup>Triple-mutant</sup>		NSP14 (A)	40	2061	1	16	178
		NSP10(B)	38	2137			
SARS-CoV	Initial structure	NSP14 (A)	42	2004	1	14	217
		NSP10 (B)	39	2182			
	Average structure from last 20 ns	<b>NSP14 (A)</b>	<b>37</b>	<b>1984</b>	<b>1</b>	<b>17</b>	<b>166</b>
		<b>NSP10 (B)</b>	<b>37</b>	<b>1913</b>			
MERS-CoV	Initial structure	NSP14 (A)	42	1797	2	8	575
		NSP10 (B)	39	1989			
	Average structure from last 20 ns	<b>NSP14 (A)</b>	<b>28</b>	<b>1689</b>	<b>1</b>	<b>11</b>	<b>129</b>
		<b>NSP10 (B)</b>	<b>31</b>	<b>1690</b>			

**Table S4.** Comparison of interface statistics of the initial NSP14-NSP10 complexes (before MD) of SARS-CoV-2, SARS-CoV and MERS-CoV with the average complex structures extracted from last 20 ns from 100 ns MD trajectory of replica 3. For each complex, interface statistics obtained from PDBsum server.

Human CoV	Time	Protein chains PPI complexes	#Interface residues	Interface area (Å <sup>2</sup> )	#Salt bridges	# H-bonds	# non-bonded contacts
SARS-CoV-2	Initial structure	NSP14 (A)	50	2135	1	22	313
		NSP10 (B)	45	2320			
	Average structure from last 20 ns	<b>NSP14 (A)</b>	<b>38</b>	<b>1937</b>	-	<b>13</b>	<b>156</b>
		<b>NSP10(B)</b>	<b>34</b>	<b>2042</b>			
SARS-CoV-2 <sup>F233L</sup>	Average structure from last 20 ns	NSP14 (A)	39	1998	1	17	174
		NSP10(B)	36	2079			
SARS-CoV-2 <sup>P203L</sup>	Average structure from last 20 ns	NSP14 (A)	37	1975	1	13	151
		NSP10(B)	31	2120			
SARS-CoV-2 <sup>L177F</sup>	Average structure from last 20 ns	NSP14 (A)	32	1772	1	8	127
		NSP10(B)	28	1907			
SARS-CoV-2 <sup>Triple-mutant</sup>	Average structure from last 20 ns	NSP14 (A)	39	1993	1	15	170
SARS-CoV	Initial structure	NSP14 (A)	42	2004	1	14	217
		NSP10 (B)	39	2182			
	Average structure from last 20 ns	<b>NSP14 (A)</b>	<b>36</b>	<b>2074</b>	<b>1</b>	<b>17</b>	<b>190</b>
		<b>NSP10 (B)</b>	<b>42</b>	<b>1972</b>			
MERS-CoV	Initial structure	NSP14 (A)	42	1797	2	8	575
		NSP10 (B)	39	1989			
	Average structure from last 20 ns	<b>NSP14 (A)</b>	<b>32</b>	<b>1639</b>	<b>2</b>	<b>11</b>	<b>140</b>
		<b>NSP10 (B)</b>	<b>32</b>	<b>1724</b>			

**Table S5.** Total number of H-bond involved in the average conformer of SARS-CoV-2 NSP14-NSP10 complex extracted from last 20 ns MD trajectory of replica 1. The interface H-bond results obtained from PDBsum server.

Sl. no.	Atom no.	Atom name	Res. Name	Res. no.	Atom Chain	Atom no.	Atom name	Res. Name	Res. no.	Atom Chain	Distance
1	72	O	LEU	7	A	4567	N	GLU	6	B	3.28
2	123	OD1	ASP	10	A	4510	N	ALA	1	B	2.63
3	290	O	THR	21	A	5833	N	GLY	94	B	3.04
4	564	O	CYS	39	A	5132	N	LEU	45	B	2.88
5	589	OD1	ASP	41	A	5317	OG1	THR	58	B	2.69
6	590	OD2	ASP	41	A	5875	OH	TYR	96	B	2.72
7	910	N	LYS	61	A	4703	OG	SER	15	B	3.3
8	1017	N	ASN	67	A	4970	OG	SER	33	B	3.03
9	1051	OH	TYR	69	A	4910	OD2	ASP	29	B	2.67
10	1938	O	THR	127	A	5827	NZ	LYS	93	B	2.77
11	3154	N	ILE	201	A	4767	O	PHE	19	B	3.07
12	3172	O	ILE	201	A	4778	N	VAL	21	B	2.88



**Table S6.** Total number of H-bond involved in the average conformer of SARS-CoV-2 NSP14-NSP10 complex extracted from last 20 ns MD trajectory of replica 2. The interface H-bond results obtained from PDBsum server.

Sl. no.	Atom no.	Atom name	Res. Name	Res. no.	Atom Chain	Atom no.	Atom name	Res. Name	Res. no.	Atom Chain	Distance
1	54	N	LEU	7	A	4581	O	GLU	6	B	3.25
2	72	O	LEU	7	A	4567	N	GLU	6	B	3.05
3	92	O	PHE	8	A	4553	N	THR	5	B	3.07
4	92	O	PHE	8	A	4559	OG1	THR	5	B	2.78
5	115	N	ASP	10	A	4542	O	ASN	3	B	3.31
6	290	O	THR	21	A	5833	N	GLY	94	B	3.31
7	338	OG1	THR	25	A	4566	O	THR	5	B	2.67
8	346	N	HIS	26	A	5065	O	ASN	40	B	3.07
9	346	N	HIS	26	A	5060	OD1	ASN	40	B	3.06
10	363	N	LEU	27	A	5060	OD1	ASN	40	B	3.22
11	554	N	CYS	39	A	5114	O	LYS	43	B	2.98
12	564	O	CYS	39	A	5132	N	LEU	45	B	2.81
13	910	N	LYS	61	A	4703	OG	SER	15	B	2.96
14	1017	N	ASN	67	A	4970	OG	SER	33	B	2.97
15	1051	OH	TYR	69	A	4910	OD2	ASP	29	B	2.88
16	1976	ND2	ASN	130	A	5748	O	GLY	88	B	2.90
17	1987	OG1	THR	131	A	5620	ND1	HIS	80	B	3.00
18	3154	N	ILE	201	A	4767	O	PHE	19	B	3.06
19	3172	O	ILE	201	A	4778	N	VAL	21	B	2.99

**Table S7.** Total number of H-bond involved in the average conformer of SARS-CoV-2 NSP14-NSP10 complex extracted from last 20 ns MD trajectory of replica 3. The interface H-bond results obtained from PDBsum server.

Sl. no.	Atom no.	Atom name	Res. Name	Res. no.	Atom Chain	Atom no.	Atom name	Res. Name	Res. no.	Atom Chain	Distance
1	33	N	THR	5	A	4581	O	GLU	6	B	2.85
2	115	N	ASP	10	A	4542	O	ASN	3	B	2.93
3	126	O	ASP	10	A	4529	N	ASN	3	B	2.86
4	331	O	PRO	24	A	5501	OG	SER	72	B	2.68
5	338	OG1	THR	25	A	4566	O	THR	5	B	2.87
6	346	N	HIS	26	A	5065	O	ASN	40	B	2.98
7	554	N	CYS	39	A	5114	O	LYS	43	B	2.94
8	564	O	CYS	39	A	5132	N	LEU	45	B	2.82
9	910	N	LYS	61	A	4703	OG	SER	15	B	3.03
10	1017	N	ASN	67	A	4970	OG	SER	33	B	3.09
11	1051	OH	TYR	69	A	4910	OD2	ASP	29	B	2.67
12	3154	N	ILE	201	A	4767	O	PHE	19	B	2.94
13	3172	O	ILE5	201	A	4778	N	VAL	21	B	2.82

**Table S8.** Total number of H-bond involved in the average conformer of SARS-CoV NSP14-NSP10 complex extracted from last 20 ns MD trajectory of replica 1. The interface H-bond results obtained from PDBsum server.

Sl. no.	Atom no.	Atom name	Res. Name	Res. no.	Chain NSP14	Atom no.	Atom name	Res. Name	Res. no.	Chain NSP10	Distance
1	2246	OG1	THR	25	A	57	O	THR	5	B	2.84
2	1951	O	THR	5	A	58	N	GLU	6	B	3.26
3	1938	N	THR	5	A	72	O	GLU	6	B	2.79
4	2844	O	LYS	61	A	194	OG	SER	15	B	2.81
5	5065	N	ILE	201	A	258	O	PHE	19	B	2.94
6	5083	O	ILE	201	A	269	N	VAL	21	B	2.89
7	2964	OH	TYR	69	A	405	OD2	ASP	29	B	2.69
8	2930	N	ASN	67	A	465	OG	SER	33	B	3.1
9	2254	N	HIS	26	A	560	O	ASN	40	B	3.06
10	2467	N	CYS	39	A	609	O	LYS	43	B	2.88
11	2477	O	CYS	39	A	627	N	LEU	45	B	2.8
12	2503	OD2	ASP	41	A	812	OG1	THR	58	B	2.77
13	3877	O	ASN	129	A	1264	N	CYS	90	B	2.87
14	3831	OD1	ASP	126	A	1322	NZ	LYS	93	B	2.64
15	3848	O	THR	127	A	1322	NZ	LYS	93	B	2.75
16	2198	O	THR	21	A	1328	N	GLY	94	B	3
17	2502	OD1	ASP	41	A	1370	OH	TYR	96	B	2.66

**Table S9.** Total number of H-bond involved in the average conformer of SARS-CoV NSP14-NSP10 complex extracted from last 20 ns MD trajectory of replica 2. The interface H-bond results obtained from PDBsum server.

Sl. no.	Atom no.	Atom name	Res. Name	Res. no.	Atom Chain	Atom no.	Atom name	Res. Name	Res. no.	Atom Chain	Distance
1	57	O	THR	5	A	2245	OG1	THR		B	2.81
2	72	O	GLU	6	A	1937	N	THR		B	2.88
3	194	OG	SER	15	A	2888	OH	TYR		B	3.17
4	258	O	PHE	19	A	5064	N	ILE		B	2.96
5	269	N	VAL	21	A	5082	O	ILE		B	3.00
6	405	OD2	ASP	29	A	2963	OH	TYR		B	2.66
7	465	OG	SER	33	A	2929	N	ASN		B	2.96
8	560	O	ASN	40	A	2253	N	HIS		B	2.88
9	609	O	LYS	43	A	2466	N	CYS		B	3.21
10	627	N	LEU	45	A	2476	O	CYS		B	2.80
11	979	N	ALA	71	A	2197	O	THR		B	3.02
12	996	OG	SER	72	A	2238	O	PRO		B	2.77
13	1264	N	CYS	90	A	3876	O	ASN		B	2.84
14	1322	NZ	LYS	93	A	3830	OD1	ASP		B	2.89
15	1322	NZ	LYS	93	A	3847	O	THR		B	2.78
16	1322	NZ	LYS	93	A	3890	O	ASN		B	3.09
17	1328	N	GLY	94	A	2209	OE1	GLN		B	2.86

**Table S10.** Total number of H-bond involved in the average conformer of SARS-CoV NSP14-NSP10 complex extracted from last 20 ns MD trajectory of replica 3. The interface H-bond results obtained from PDBsum server.

Sl. no.	Atom no.	Atom name	Res. Name	Res. no.	Atom Chain	Atom no.	Atom name	Res. Name	Res. no.	Atom Chain	Distance
1	2028	OD2	ASP	10	A	1	N	ALA	1	B	2.54
2	2019	N	ASP	10	A	33	O	ASN	3	B	2.93
3	1996	O	PHE	8	A	44	N	THR	5	B	2.90
4	2245	OG1	THR	25	A	57	O	THR	5	B	2.67
5	5064	N	ILE	201	A	258	O	PHE	19	B	3.09
6	5082	O	ILE	201	A	269	N	VAL	21	B	2.84
7	2963	OH	TYR	69	A	405	OD2	ASP	29	B	2.68
8	2929	N	ASN	67	A	465	OG	SER	33	B	3.07
9	2253	N	HIS	26	A	560	O	ASN	40	B	3.03
10	2466	N	CYS	39	A	609	O	LYS	43	B	2.90
11	2476	O	CYS	39	A	627	N	LEU	45	B	2.80
12	2197	O	THR	21	A	979	N	ALA	71	B	3.24
13	2238	O	PRO	24	A	996	OG	SER	72	B	2.69
14	3891	N	THR	131	A	1243	O	GLY	88	B	3.19
15	3830	OD1	ASP	126	A	1322	NZ	LYS	93	B	2.65
16	3847	O	THR	127	A	1322	NZ	LYS	93	B	2.81
17	2209	OE1	GLN	22	A	1328	N	GLY	94	B	2.90

**Table S11.** Total number of H-bond involved in the average conformer of MERS-CoV NSP14-NSP10 complex extracted from last 20 ns MD trajectory of replica 1. The interface H-bond results obtained from PDBsum server.

Sl. no.	Atom no.	Atom name	Res. Name	Res. no.	Atom Chain	Atom no.	Atom name	Res. Name	Res. no.	Atom Chain	Distance
1	306	O	ALA	21	A	5697	N	GLY	94	B	3.07
2	366	N	TYR	26	A	4912	O	ASN	40	B	2.97
3	590	N	CYS	40	A	4961	O	LYS	43	B	2.95
4	600	O	CYS	40	A	4979	N	LEU	45	B	2.8
5	921	N	LYS	61	A	4538	OG	SER	15	B	3.09
6	1919	OD2	ASP	126	A	5691	NZ	LYS	93	B	2.54
7	1935	O	THR	127	A	5691	NZ	LYS	93	B	2.82
8	1974	O	TRP	129	A	5621	N	CYS	90	B	2.9
9	1991	ND2	ASN	131	A	5484	ND1	HIS	80	B	3.04
10	3097	N	ILE	201	A	4610	O	PHE	19	B	2.94

**Table S12.** Total number of H-bond involved in the average conformer of MERS-CoV NSP14-NSP10 complex extracted from last 20 ns MD trajectory of replica 2. The interface H-bond results obtained from PDBsum server.

Sl. no.	Atom no.	Atom name	Res. Name	Res. no.	Atom Chain	Atom no.	Atom name	Res. Name	Res. no.	Atom Chain	Distance
1	306	O	ALA	21	A	5697	N	GLY	94	B	2.99
2	379	OH	TYR	26	A	4940	N	LYS	43	B	3.03
3	590	N	CYS	40	A	4961	O	LYS	43	B	3.03
4	600	O	CYS	40	A	4979	N	LEU	45	B	2.81
5	921	N	LYS	61	A	4538	OG	SER	15	B	3.13
6	1048	OH	TYR	69	A	4765	OD2	ASP	29	B	2.65
7	1974	O	TRP	129	A	5621	N	CYS	90	B	2.83
8	1990	OD1	ASN	131	A	5539	NE2	HIS	83	B	2.84
9	1991	ND2	ASN	131	A	5512	O	ILE	81	B	2.95
10	3097	N	ILE	201	A	4610	O	PHE	19	B	2.84
11	3115	O	ILE	201	A	4625	N	VAL	21	B	2.86

**Table S13.** Total number of H-bond involved in the average conformer of MERS-CoV NSP14-NSP10 complex extracted from last 20 ns MD trajectory of replica 3. The interface H-bond results obtained from PDBsum server.

Sl. no.	Atom no.	Atom name	Res. Name	Res. no.	Atom Chain	Atom no.	Atom name	Res. Name	Res. no.	Atom Chain	Distance
1	306	O	ALA	21	A	5697	N	GLY	94	B	3.10
2	590	N	CYS	40	A	4961	O	LYS	43	B	3.23
3	600	O	CYS	40	A	4979	N	LEU	45	B	2.83
4	869	NH1	ARG	57	A	5476	O	ALA	79	B	3.19
5	921	N	LYS	61	A	4538	OG	SER	15	B	2.91
6	1935	O	THR	127	A	5691	NZ	LYS	93	B	2.80
7	1974	O	TRP	129	A	5621	N	CYS	90	B	3.03
8	1981	O	GLY	130	A	5691	NZ	LYS	93	B	3.02
9	1991	ND2	ASN	131	A	5512	O	ILE	81	B	3.00
10	3097	N	ILE	201	A	4610	O	PHE	19	B	3.15
11	3115	O	ILE	201	A	4625	N	VAL	21	B	2.92



**Table S14.** Total number of H-bond involved in the average conformer of SARS-CoV-2 NSP14<sup>L177F</sup> mutant complex extracted from last 20 ns MD trajectory of replica 1. The interface H-bond results obtained from PDBsum server.

Sl No.	Atom no.	Atom name	Res. name	Res no.	Chain NSP12	Atom no.	Atom name	Res. name	Res no.	Chain NSP8	Distance
1	290	O	THR	21	A	5834	N	GLY	94	B	3.08
2	564	O	CYS	39	A	5133	N	LEU	45	B	2.83
3	910	N	LYS	61	A	4704	OG	SER	15	B	3.04
4	1017	N	ASN	67	A	4971	OG	SER	33	B	2.99
5	1051	OH	TYR	69	A	4911	OD2	ASP	29	B	2.67
6	1922	OD2	ASP	126	A	5828	NZ	LYS	93	B	2.77
7	1938	O	THR	127	A	5828	NZ	LYS	93	B	2.77
8	1966	O	ASN	129	A	5770	N	CYS	90	B	2.94
9	3155	N	ILE	201	A	4768	O	PHE	19	B	3.05
10	3173	O	ILE	201	A	4779	N	VAL	21	B	2.82

**Table S15.** Total number of H-bond involved in the average conformer of SARS-CoV-2 NSP14<sup>L177F</sup> mutant complex extracted from last 20 ns MD trajectory of replica 2. The interface H-bond results obtained from PDBsum server.

Sl. no.	Atom no.	Atom name	Res. Name	Res. no.	Atom Chain	Atom no.	Atom name	Res. Name	Res. no.	Atom Chain	Distance
1	33	N	THR	5	A	4582	O	GLU	6	B	2.86
2	115	N	ASP	10	A	4543	O	ASN	3	B	2.89
3	126	O	ASP	10	A	4530	N	ASN	3	B	2.92
4	564	O	CYS	39	A	5133	N	LEU	45	B	2.86
5	589	OD1	ASP	41	A	5318	OG1	THR	58	B	3.03
6	590	OD2	ASP	41	A	5876	OH	TYR	96	B	3.10
7	910	N	LYS	61	A	4704	OG	SER	15	B	3.06
8	1017	N	ASN	67	A	4971	OG	SER	33	B	2.94
9	1051	OH	TYR	69	A	4910	OD1	ASP	29	B	2.96
10	1922	OD2	ASP	126	A	5828	NZ	LYS	93	B	2.89
11	1966	O	ASN	129	A	5770	N	CYS	90	B	2.97
12	1962	ND2	ASN	129	A	5833	O	LYS	93	B	3.22
13	3155	N	ILE	201	A	4768	O	PHE	19	B	3.06
14	3173	O	ILE	201	A	4779	N	VAL	21	B	3.00

**Table S16.** Total number of H-bond involved in the average conformer of SARS-CoV-2 NSP14<sup>L177F</sup> mutant complex extracted from last 20 ns MD trajectory of replica 3. The interface H-bond results obtained from PDBsum server.

Sl. no.	Atom no.	Atom name	Res. Name	Res. no.	Atom Chain	Atom no.	Atom name	Res. Name	Res. no.	Atom Chain	Distance
1	338	OG1	THR	25	A	4567	O	THR	5	B	2.80
2	346	N	HIS	26	A	5061	OD1	ASN	40	B	2.95
3	554	N	CYS	39	A	5115	O	LYS	43	B	3.16
4	564	O	CYS	39	A	5133	N	LEU	45	B	2.79
5	910	N	LYS	61	A	4704	OG	SER	15	B	3.00
6	1017	N	ASN	67	A	4971	OG	SER	33	B	2.93
7	3155	N	ILE	201	A	4768	O	PHE	19	B	3.07
8	3173	O	ILE	201	A	4779	N	VAL	21	B	2.91

**Table S17.** Total number of H-bond involved in the average conformer of SARS-CoV-2 NSP14<sup>P230L</sup> mutant complex extracted from last 20 ns MD trajectory of replica 1. The interface H-bond results obtained from PDBsum server.

Sl. No	Atom no.	Atom name	Res. name	Res no.	Chain NSP14	Atom no.	Atom name	Res. name	Res no.	Chain NSP10	Distance
1	290	O	THR	21	A	5838	N	GLY	94	B	3.07
2	331	O	PRO	24	A	5506	OG	SER	72	B	2.71
3	338	OG1	THR	25	A	4571	O	THR	5	B	2.73
4	346	N	HIS	26	A	5070	O	ASN	40	B	2.97
5	554	N	CYS	39	A	5119	O	LYS	43	B	3.05
6	564	O	CYS	39	A	5137	N	LEU	45	B	2.81
7	590	OD2	ASP	41	A	5880	OH	TYR	96	B	3.2
8	910	N	LYS	61	A	4708	OG	SER	15	B	3.06
9	1017	N	ASN	67	A	4975	OG	SER	33	B	2.96
10	1051	OH	TYR	69	A	4915	OD2	ASP	29	B	2.65
11	1966	O	ASN	129	A	5774	N	CYS	90	B	3.02
12	3154	N	ILE	201	A	4772	O	PHE	19	B	3.08
13	3172	O	ILE	201	A	4783	N	VAL	21	B	2.94

**Table S18.** Total number of H-bond involved in the average conformer of SARS-CoV-2 NSP14<sup>P230L</sup> mutant complex extracted from last 20 ns MD trajectory of replica 2. The interface H-bond results obtained from PDBsum server

Sl. no.	Atom no.	Atom name	Res. Name	Res. no.	Atom Chain	Atom no.	Atom name	Res. Name	Res. no.	Atom Chain	Distance
1	33	N	THR	5	A	4586	O	GLU	6	B	2.84
2	115	N	ASP	10	A	4547	O	ASN	3	B	3.01
3	126	O	ASP	10	A	4534	N	ASN	3	B	2.96
4	290	O	THR	21	A	5838	N	GLY	94	B	3.19
5	338	OG1	THR	25	A	4571	O	THR	5	B	2.73
6	346	N	HIS	26	A	5070	O	ASN	40	B	3.10
7	353	ND1	HIS	26	A	5098	N	LYS	43	B	3.33
8	554	N	CYS	39	A	5119	O	LYS	43	B	2.88
9	564	O	CYS	39	A	5137	N	LEU	45	B	2.79
10	590	OD2	ASP	41	A	5880	OH	TYR	96	B	2.94
11	910	N	LYS	61	A	4708	OG	SER	15	B	3.03
12	1017	N	ASN	67	A	4975	OG	SER	33	B	3.03
13	1051	OH	TYR	69	A	4915	OD2	ASP	29	B	2.65
14	3154	N	ILE	201	A	4772	O	PHE	19	B	2.97
15	3172	O	ILE	201	A	4783	N	VAL	21	B	2.86

**Table S19.** Total number of H-bond involved in the average conformer of SARS-CoV-2 NSP14<sup>P230L</sup> mutant complex extracted from last 20 ns MD trajectory of replica 3. The interface H-bond results obtained from PDBsum server

Sl. no.	Atom no.	Atom name	Res. Name	Res. no.	Atom Chain	Atom no.	Atom name	Res. Name	Res. no.	Atom Chain	Distance
1	33	N	THR	5	A	4586	O	GLU	6	B	2.84
2	115	N	ASP	10	A	4547	O	ASN	3	B	2.96
3	126	O	ASP	10	A	4534	N	ASN	3	B	2.83
4	290	O	THR	21	A	5838	N	GLY	94	B	3.09
5	338	OG1	THR	25	A	4564	OG1	THR	5	B	2.78
6	389	OG	SER	28	A	4564	OG1	THR	5	B	2.83
7	564	O	CYS	39	A	5137	N	LEU	45	B	2.92
8	589	OD1	ASP	41	A	5880	OH	TYR	96	B	2.93
9	910	N	LYS	61	A	4708	OG	SER	15	B	3.00
10	1051	OH	TYR	69	A	4914	OD1	ASP	29	B	2.66
11	1922	OD2	ASP	126	A	5832	NZ	LYS	93	B	2.71
12	3154	N	ILE	201	A	4772	O	PHE	19	B	3.02
13	3172	O	ILE	201	A	4783	N	VAL	21	B	3.20

**Table S20.** Total number of H-bond involved in the average conformer of SARS-CoV-2 NSP14<sup>F233L</sup> mutant complex extracted from last 20 ns MD trajectory of replica 1. The interface H-bond results obtained from PDBsum server.

Sl No.	Atom no.	Atom name	Res. name	Res no.	Chain NSP14	Atom no.	Atom name	Res. name	Res no.	Chain NSP10	Distance
1	33	N	THR	5	A	4580	O	GLU	6	B	2.89
2	115	N	ASP	10	A	4541	O	ASN	3	B	3.16
3	126	O	ASP	10	A	4528	N	ASN	3	B	3.3
4	290	O	THR	21	A	5832	N	GLY	94	B	3.11
5	331	O	PRO	24	A	5500	OG	SER	72	B	2.72
6	338	OG1	THR	25	A	4565	O	THR	5	B	2.89
7	346	N	HIS	26	A	5064	O	ASN	40	B	3.04
8	554	N	CYS	39	A	5113	O	LYS	43	B	3.11
9	564	O	CYS	39	A	5131	N	LEU	45	B	2.82
10	589	OD1	ASP	41	A	5316	OG1	THR	58	B	3.26
11	590	OD2	ASP	41	A	5874	OH	TYR	96	B	3.16
12	910	N	LYS	61	A	4702	OG	SER	15	B	3.00
13	1017	N	ASN	67	A	4969	OG	SER	33	B	3.00
14	1051	OH	TYR	69	A	4909	OD2	ASP	29	B	2.67
15	1921	OD1	ASP	126	A	5826	NZ	LYS	93	B	2.69
16	3154	N	ILE	201	A	4766	O	PHE	19	B	3.03
17	3172	O	ILE	201	A	4777	N	VAL	21	B	2.93

**Table S21.** Total number of H-bond involved in the average conformer of SARS-CoV-2 NSP14<sup>F233L</sup> mutant complex extracted from last 20 ns MD trajectory of replica 2. The interface H-bond results obtained from PDBsum server.

Sl. no.	Atom no.	Atom name	Res. Name	Res. no.	Atom Chain	Atom no.	Atom name	Res. Name	Res. no.	Atom Chain	Distance
1	33	N	THR	5	A	4580	O	GLU	6	B	3.09
2	92	O	PHE	8	A	4558	OG1	THR	5	B	2.83
3	115	N	ASP	10	A	4541	O	ASN	3	B	2.91
4	331	O	PRO	24	A	5500	OG	SER	72	B	2.71
5	338	OG1	THR	25	A	4565	O	THR	5	B	2.68
6	346	N	HIS	26	A	5064	O	ASN	40	B	2.90
7	363	N	LEU	27	A	5059	OD1	ASN	40	B	3.29
8	554	N	CYS	39	A	5113	O	LYS	43	B	2.88
9	564	O	CYS	39	A	5131	N	LEU	45	B	2.83
10	910	N	LYS	61	A	4702	OG	SER	15	B	3.01
11	1017	N	ASN	67	A	4969	OG	SER	33	B	3.04
12	1051	OH	TYR	69	A	4908	OD1	ASP	29	B	2.66
13	3154	N	ILE	201	A	4766	O	PHE	19	B	2.97
14	3172	O	ILE	201	A	4777	N	VAL	21	B	2.82



**Table S22.** Total number of H-bond involved in the average conformer of SARS-CoV-2 NSP14<sup>F233L</sup> mutant complex extracted from last 20 ns MD trajectory of replica 3. The interface H-bond results obtained from PDBsum server.

Sl no.	Atom no.	Atom name	Res name	Res no.	Atom Chain	Atom no.	Atom name	Res. name	Res. no.	Atom Chain	Distance
1.	33	N	THR	5	A	4580	O	GLU	6	B	3.04
2.	115	N	ASP	10	A	4541	O	ASN	3	B	2.94
3.	126	O	ASP	10	A	4528	N	ASN	3	B	2.84
4.	290	O	THR	21	A	5832	N	GLY	94	B	3.11
5.	338	OG1	THR	25	A	4565	O	THR	5	B	2.73
6.	346	N	HIS	26	A	5059	OD1	ASN	40	B	3.26
7.	554	N	CYS	39	A	5113	O	LYS	43	B	3.21
8.	564	O	CYS	39	A	5131	N	LEU	45	B	2.91
9.	590	OD2	ASP	41	A	5874	OH	TYR	96	B	3.07
10.	910	N	LYS	61	A	4702	OG	SER	15	B	3.09
11.	1017	N	ASN	67	A	4969	OG	SER	33	B	3.00
12.	1051	OH	TYR	69	A	4909	OD2	ASP	29	B	2.71
13.	1921	OD1	ASP	126	A	5826	NZ	LYS	93	B	2.90
14.	1922	OD2	ASP	126	A	5826	NZ	LYS	93	B	2.81
15.	1966	O	ASN	129	A	5768	N	CYS	90	B	2.88
16.	3154	N	ILE	201	A	4766	O	PHE	19	B	3.03
17.	3172	O	ILE	201	A	4777	N	VAL	21	B	2.92

**Table S23.** Total number of H-bond involved in the average conformer of SARS-CoV-2 NSP14<sup>Triple</sup> mutant complex extracted from last 20 ns MD trajectory of replica 1. The interface H-bond results obtained from PDBsum server.

Sl No.	Atom no.	Atom name	Res. name	Res no.	Chain NSP12	Atom no.	Atom name	Res. name	Res no.	Chain NSP8	Distance
1	33	N	THR	5	A	4586	O	GLU	6	B	2.91
2	92	O	PHE	8	A	4564	OG1	THR	5	B	3.18
3	115	N	ASP	10	A	4547	O	ASN	3	B	2.88
4	126	O	ASP	10	A	4534	N	ASN	3	B	2.9
5	290	O	THR	21	A	5838	N	GLY	94	B	3.13
6	331	O	PRO	24	A	5506	OG	SER	72	B	2.7
7	338	OG1	THR	25	A	4571	O	THR	5	B	2.72
8	346	N	HIS	26	A	5070	O	ASN	40	B	3
9	554	N	CYS	39	A	5119	O	LYS	43	B	3.1
10	564	O	CYS	39	A	5137	N	LEU	45	B	2.85
11	910	N	LYS	61	A	4708	OG	SER	15	B	2.98
12	1017	N	ASN	67	A	4975	OG	SER	33	B	2.99
13	1051	OH	TYR	69	A	4914	OD1	ASP	29	B	2.67
14	1922	OD2	ASP	126	A	5832	NZ	LYS	93	B	2.89
15	1976	ND2	ASN	130	A	5753	O	GLY	88	B	2.95
16	3155	N	ILE	201	A	4772	O	PHE	19	B	3.01
17	3173	O	ILE	201	A	4783	N	VAL	21	B	2.86

**Table S24.**Total number of H-bond involved in the average conformer of SARS-CoV-2 NSP14<sup>Triple</sup> mutant complex extracted from last 20 ns MD trajectory of replica 2. The interface H-bond results obtained from PDBsum server.

Sl. no.	Atom no.	Atom name	Res. Name	Res. no.	Atom Chain	Atom no.	Atom name	Res. Name	Res. no.	Atom Chain	Distance
1	33	N	THR	5	A	4586	O	GLU	6	B	2.93
2	92	O	PHE	8	A	4564	OG1	THR	5	B	3.27
3	115	N	ASP	10	A	4547	O	ASN	3	B	2.92
4	126	O	ASP	10	A	4534	N	ASN	3	B	2.85
5	290	O	THR	21	A	5838	N	GLY	94	B	3.24
6	338	OG1	THR	25	A	4571	O	THR	5	B	2.76
7	346	N	HIS	26	A	5070	O	ASN	40	B	2.98
8	564	O	CYS	39	A	5137	N	LEU	45	B	2.82
9	589	OD1	ASP	41	A	5322	OG1	THR	58	B	2.63
10	590	OD2	ASP	41	A	5880	OH	TYR	96	B	2.69
11	910	N	LYS	61	A	4708	OG	SER	15	B	3.04
12	1017	N	ASN	67	A	4975	OG	SER	33	B	3.04
13	1051	OH	TYR	69	A	4915	OD2	ASP	29	B	2.67
14	1922	OD2	ASP	126	A	5832	NZ	LYS	93	B	2.69
15	3155	N	ILE	201	A	4772	O	PHE	19	B	2.93
16	3173	O	ILE	201	A	4783	N	VAL	21	B	2.85

**Table S25.** Total number of H-bond involved in the average conformer of SARS-CoV-2 NSP14<sup>Triple</sup> mutant complex extracted from last 20 ns MD trajectory of replica 3. The interface H-bond results obtained from PDBsum server.

Sl no.	Atom no.	Atom name	Res name	Res no.	Atom Chain	Atom no.	Atom name	Res. name	Res. no.	Atom Chain	Distance
1.	33	N	THR	5	A	4586	O	GLU	6	B	2.89
2.	115	N	ASP	10	A	4547	O	ASN	3	B	2.92
3.	126	O	ASP	10	A	4534	N	ASN	3	B	2.82
4.	290	O	THR	21	A	5838	N	GLY	94	B	3.29
5.	338	OG1	THR	25	A	4571	O	THR	5	B	2.72
6.	346	N	HIS	26	A	5065	OD1	ASN	40	B	2.99
7.	363	N	LEU	27	A	5065	OD1	ASN	40	B	3.30
8.	554	N	CYS	39	A	5119	O	LYS	43	B	2.93
9.	564	O	CYS	39	A	5137	N	LEU	45	B	2.80
10.	910	N	LYS	61	A	4708	OG	SER	15	B	3.02
11.	1017	N	ASN	67	A	4975	OG	SER	33	B	2.98
12.	1051	OH	TYR	69	A	4914	OD1	ASP	29	B	2.65
13.	1922	OD2	ASP	126	A	5832	NZ	LYS	93	B	2.64
14.	3155	N	ILE	201	A	4772	O	PHE	19	B	3.00
15.	3173	O	ILE	201	A	4783	N	VAL	21	B	2.96

**Table S26.** Total number of H-bond involved in the initial structure (before MD) of SARS-CoV-2 NSP14-NSP10 PPI complex interface obtained from PDBsum server

Sl. no.	Atom no.	Atom name	Res. Name	Res. no.	Atom Chain	Atom no.	Atom name	Res. Name	Res. no.	Atom Chain	Distance
1	16	N	THR	5	A	2337	O	GLU	6	M	3.04
2	38	O	PHE	8	A	2332	OG1	THR	5	M	2.76
3	54	NZ	LYS	9	A	2308	O	ALA	1	M	2.79
4	55	N	ASP	10	A	2317	O	ASN	3	M	2.82
5	58	O	ASP	10	A	2314	N	ASN	3	M	2.84
6	146	O	THR	21	A	2988	N	GLY	94	M	2.84
7	176	OG1	THR	25	A	2330	O	THR	5	M	2.64
8	178	N	HIS	26	A	2590	O	ASN	40	M	2.94
9	281	N	CYS	39	A	2611	O	LYS	43	M	3.06
10	284	O	CYS	39	A	2625	N	LEU	45	M	2.75
11	300	OD1	ASP	41	A	3012	OH	TYR	96	M	2.6
12	463	N	LYS	61	A	2403	OG	SER	15	M	2.94
13	486	OD1	ASN	63	A	2381	OG1	THR	12	M	2.63
14	516	N	ASN	67	A	2547	OG	SER	33	M	2.82
15	539	OH	TYR	69	A	2516	OD2	ASP	29	M	2.61
16	984	OD1	ASP	126	A	2881	ND1	HIS	80	M	2.81
17	989	O	THR	127	A	2987	NZ	LYS	93	M	2.48
18	1008	N	ASN	130	A	2945	O	GLY	88	M	3.17
19	1015	ND2	ASN	130	A	2907	ND1	HIS	83	M	2.85
20	1558	NZ	LYS	196	A	2424	O	ALA	18	M	2.9
21	1598	N	ILE	201	A	2429	O	PHE	19	M	2.93
22	1601	O	ILE	201	A	2442	N	VAL	21	M	2.92

**Table S27.** Total number of H-bond involved in the initial structure (before MD) of SARS-CoV NSP14-NSP10 PPI complex interface obtained from PDBsum server

Sl. no.	Atom no.	Atom name	Res. Name	Res. no.	Atom Chain	Atom no.	Atom name	Res. Name	Res. no.	Atom Chain	Distance
1	1028	NZ	LYS	9	A	4	O	ALA	1	B	2.54
2	1032	O	ASP	10	A	10	N	ASN	3	B	3.06
3	1029	N	ASP	10	A	13	O	ASN	3	B	2.86
4	1143	OG1	THR	25	A	26	O	THR	5	B	3.05
5	990	N	THR	5	A	33	O	GLU	6	B	2.63
6	1415	O	PHE	60	A	99	OG	SER	15	B	2.85
7	2543	N	ILE	201	A	125	O	PHE	19	B	3.14
8	2546	O	ILE	201	A	138	N	VAL	21	B	2.89
9	1145	N	HIS	26	A	281	O	ASN	40	B	3.19
10	1249	N	CYS	39	A	302	O	LYS	43	B	3.04
11	1935	OD1	ASP	126	A	572	ND1	HIS	80	B	2.66
12	1956	O	ASN	129	A	648	N	CYS	90	B	3.34
13	1347	OH	TYR	51	A	678	NZ	LYS	93	B	2.96
14	1940	O	THR	127	A	678	NZ	LYS	93	B	2.65

**Table S28.** Total number of H-bond involved in the initial structure (before MD) of MERS-CoV NSP14-NSP10 PPI complex interface obtained from PDBsum server

Sl. no.	Atom no.	Atom name	Res. Name	Res. no.	Atom Chain	Atom no.	Atom name	Res. Name	Res. no.	Atom Chain	Distance
1	164	OH	TYR	22	A	2886	O	LYS	93	B	3.16
2	182	OG1	THR	25	A	2500	O	ASN	40	B	3.23
3	303	O	CYS	40	A	2535	N	LEU	45	B	3.2
4	390	OH	TYR	51	A	2891	NZ	LYS	93	B	1.75
5	451	O	GLY	59	A	2289	OG	SER	11	B	3.3
6	984	O	TRP	129	A	2860	N	CYS	90	B	2.98
7	1559	O	ILE	201	A	2356	OG1	THR	20	B	2.73
8	1576	NZ	LYS	203	A	2430	OD2	ASP	29	B	3.23

**Table S29.** Salt bridge involved in the initial structure (before MD) of SARS-CoV-2, SARS-CoV and MERS-CoV of NSP14-NSP10 PPI complex. The salt bridges atom-atom interaction at PPI interface obtained from PDBsum server

	<b>Atom no.</b>	<b>Atom name</b>	<b>Res. Name</b>	<b>Res. no.</b>	<b>Atom Chain</b>		<b>Atom no.</b>	<b>Atom name</b>	<b>Res. Name</b>	<b>Res. no.</b>	<b>Atom Chain</b>	<b>Distance</b>
SARSCoV-2	984	OD1	ASP	126	A		2881	ND1	HIS	80	B	2.81
SARS-CoV	1935	OD1	ASP	126	A		572	ND1	HIS	80	B	2.66
MERS-CoV	963	OD1	ASP	126	A		2793	NE2	HIS	80	B	3.13
	1576	NZ	LYS	203	A		2430	OD2	ASP	29	B	3.23



**Table S30.** Salt bridge involved in the average conformer (from last 20 ns trajectory) of SARS-CoV-2, SARS-CoV and MERS-CoV NSP14-NSP10 complex extracted from last 20 ns MD trajectory from all the three sets of MD simulations. The salt bridge atom-atom interactions across protein-protein interface results are obtained from PDBsum server. In SARS-CoV-2 MD simulation replica 2 and 3, and SARS-CoV-2<sup>F233L</sup> replica 2 does not form salt bridges.

Coronaviruses	Atom no.	Atom name	Res. Name	Res. no.	Atom Chain		Atom no.	Atom name	Res. Name	Res. no.	Atom Chain	Distance
SARS-CoV-2 replica1	1921	OD1	ASP	126	A		5827	NZ	LYS	93	B	3.2
SARS-CoV- replica 1	3831	OD1	ASP	126	A		1322	NZ	LYS	93	B	2.64
SARS-CoV replica 2	1322	NZ	LYS	93	A		3830	OD1	ASP	126	B	2.89
SARS-CoV replica 3	3830	OD1	ASP	126	A		1322	NZ	LYS	93	B	2.65
MERS-CoV replica 1	1919	OD2	ASP	126	A		5691	NZ	LYS	93	B	2.54
MERS-CoV replica 2	1918	OD1	ASP	126	A		5691	NZ	LYS	93	B	2.98
MERS-CoV replica 3	1919	OD2	ASP	126	A		5488	NE2	HIS	80	B	3.50
	1918	OD2	ASP	126	A		5691	NZ	LYS	93	B	3.22
SARS-CoV-2 <sup>L177F</sup> replica 1	1922	OD2	ASP	126	A		5832	NZ	LYS	93	B	3.05
SARS-CoV-2 <sup>F233L</sup> replica 1	1921	OD1	ASP	126	A		5826	NZ	LYS	93	B	2.69
SARS-CoV-2 <sup>P203L</sup> replica 1	1922	OD2	ASP	126	A		5828	NZ	LYS	93	B	2.77
SARS-CoV-2 <sup>Triple mut</sup> replica 1	1922	OD2	ASP	126	A		5832	NZ	LYS	93	B	2.89
SARS-CoV-2 <sup>L177F</sup> replica 2	1922	OD2	ASP	126	A		5828	NZ	LYS	93	B	2.89
SARS-CoV-2 <sup>F233L</sup> replica 2	No salt bridge											
SARS-CoV-2 <sup>P203L</sup> replica 2	1921	OD2	ASP	126	A		5832	NZ	LYS	93	B	3.02
SARS-CoV-2 <sup>Triple mut</sup> replica 2	1922	OD2	ASP	126	A		5832	NZ	LYS	93	B	2.69
SARS-CoV-2 <sup>L177F</sup> replica 3	1922	OD2	ASP	126	A		5828	NZ	LYS	93	B	3.23
SARS-CoV-2 <sup>F233L</sup> replica 3	1922	OD2	ASP	126	A		5826	NZ	LYS	93	B	2.81
SARS-CoV-2 <sup>P203L</sup> replica 3	1922	OD2	ASP	126	A		5832	NZ	LYS	93	B	2.71
SARS-CoV-2 <sup>Triple-mut</sup> replica 3	1922	OD2	ASP	126	A		5832	NZ	LYS	93	B	2.64

**Table S31.** List of interacting residues at protein-protein interacting interface of SARS-CoV-2 NSP14 (Chain A) and NSP10 (Chain B), interface hotspot residues are predicted using three computational methods implemented in KFC, DrugScore<sup>PPI</sup> and Robetta web server. The per-residue energy decomposition analysis was carried out using the last 20 ns MD trajectory.

<b>Residues</b>	<b>KFC</b>	<b>Robetta <math>\Delta\Delta G</math> (kcal/mol)</b>	<b>DrugScore PPI <math>\Delta\Delta G</math> (kcal/mol)</b>	<b>Per-residue energy contribution (kJ/mol)</b>
GLY-6 A				-0.89
<b>LEU-7A</b>	<b>HS</b>	0.71	0.65	-6.5
PHE-8A	HS	2.88	1.08	-15.76
<b>ASP-10A</b>			2.02	-3.97
SER-12A				-2.93
VAL-14A				-1.62
HIS-19A		0.86		-4.03
PRO-20A	HS			-3.58
<b>THR-21A</b>	HS	1.16	0.54	-9.06
GLN-22A	HS		0.02	-2.67
ALA-23A	HS			-0.37
PRO-24A	HS			-9.07
THR-25A		0.80		-5.22
HIS-26A				-2.24
LEU-27A				-8.93
LEU-38A		1.30		-10.78
CYS-39A	HS	-0.12		-3.45
VAL-40A				-5.72
<b>ASP-41A</b>	HS	3.81	3.49	14.47
PHE-60A	HS	1.53	0.56	-9.73
<b>LYS-61A</b>				-1.11
MET-62A	HS	1.11	0.46	-10.24
TYR-64A		1.14	1.27	-7.46
VAL-66A	HS	1.58	1.89	-11.93
<b>ASN-67A</b>				-1.54
<b>TYR-69A</b>		2.69	2.33	-8.95
Met72	HS		0.12	
ASP-126A		1.01		0.65
<b>THR-127A</b>				-3.3
PRO-128A				-0.19
ASN-129A				-6.45
ASN-130A	HS	0.36	1.03	1.58
THR-131A	HS	0.60	0.45	5.11
LEU-192A				-0.24
LYS-196A				-1.31
LYS-200A				-21.5
<b>ILE-201A</b>	HS	1.61	2.03	-6.71
PHE-217A				-2.06
<b>ALA-1B</b>				94.63
ASN-3B		1.83	-0.35	3.34
ALA-4B	HS			-2.41

THR-5B	HS	1.38	0.44	-5.48
GLU-6B				-56.88
SER-11B				4.98
THR-12B				-2.33
LEU-14B	HS		0.23	-2.78
<b>SER-15B</b>	HS		0.51	-1.62
PHE-16B	HS	3.23	1.07	-16.49
ALA-18B	HS			-2.51
<b>PHE-19B</b>	HS	4.55	1.34	-4.03
ALA-20B				-5.32
<b>VAL-21B</b>		1.19	1.21	-13.16
ALA-26B				-2.62
<b>ASP-29B</b>			1.13	-49.77
TYR-30B				-4.16
<b>SER-33B</b>		1.31	0.53	1.16
VAL-42B	HS	1.48	1.12	-11.8
LYS-43B				31.59
MET-44B		1.25	0.55	-14.07
<b>LEU-45B</b>				-7.81
<b>THR-58B</b>				-2.85
PRO-59B				-2.55
GLY-69B	HS			-1.97
ALA-71B	HS			-5.37
SER-72B	HS	-0.15		-1.1
ARG-78B	HS	0.32	0.84	47.97
CYS-79B	HS		0.08	-2.59
<b>HIS-80B</b>	HS	1.47	0.17	-1.83
ILE-81B				3.24
HIS-83B				-3.18
CYS-90B				-4.54
<b>LYS-93B</b>	HS	3.49	1.55	88.01
<b>GLY-94B</b>				-2.46
LYS-95B				38.03
<b>TYR-96B</b>	HS	5.34	3.07	-5.54

---

\*HS: Hotspot; Predicted HS depicted in red; H-bond forming residues depicted in blue

**Table S32.** List of interacting residues at protein-protein interacting interface of SARS-CoV NSP14 (Chain A) and NSP10 (Chain B), interface hotspot residues are predicted using three computational methods implemented in KFC, DrugScore<sup>PPI</sup> and Robetta web server. The per-residue energy decomposition analysis was carried out using the last 20 ns MD trajectory.

Residues	KFC	Robetta $\Delta\Delta G$ (kcal/mol)	DrugScore PPI $\Delta\Delta G$ (kcal/mol)	Per-residue energy contribution (kJ/mol)
ASN-3A				1.07
VAL-4A		1.05	1.28	-11.36
<b>THR-5A</b>	HS	1.04	0.41	-9.63
GLY-6A				-2.1
LEU-7A	HS	2.07	1.31	-16.56
PHE-8A	HS	2.10	0.62	-13.63
LYS-9A				-0.22
ASP-10A				5.68
PRO-20A	HS			-4.06
<b>THR-21A</b>	HS	0.74	0.45	-10.65
GLN-22A				-5.36
ALA-23A	HS			-0.41
PRO-24A	HS			-9.81
<b>THR-25A</b>	HS	2.49	0.85	-14.09
<b>HIS-26A</b>				-6.44
LEU-27A				-10.71
SER-28A	HS	0.93	0.24	-2.87
VAL-29A				-4.49
LEU-38A		1.29	1.13	-14.12
<b>CYS-39A</b>	HS	-0.13	0.31	-5.37
VAL-40A				-6.85
<b>ASP-41A</b>		1.25	3.52	23.56
TYR-51A			0.60	-2.52
ILE-55A	HS	0.64	0.93	-4.54
PHE-60A	HS	0.82	0.29	-2.3
<b>LYS-61A</b>				-6.75
MET-62A	HS	1.14	0.53	-11.56
TYR-64A		0.92	0.91	-9.21
VAL-66A	HS	1.58	1.94	-15.78
<b>ASN-67A</b>				-1.25
<b>TYR-69A</b>	HS	3.35	2.54	-10.15
<b>ASP-126A</b>	HS	0.72	0.61	12.15
THR-127A				-4.58
GLU-128A				-16.74
<b>ASN-129A</b>				-5.47
ASN-130A				-9.01
THR-131A	HS	0.73	0.38	6.76
LYS-196A	HS	-0.21	0.25	9.88
LYS-200A				
<b>ILE-201A</b>	HS	0.70	0.94	-5.61
PHE-217A				-3.79
ALA-1B				51.51

ASN-3B				1.41
ALA-4B				-5.82
<b>THR-5B</b>	HS	0.02	0.34	-4.02
<b>GLU-6B</b>	HS	7.92	-0.61	-18.3
PRO-8B				-10.07
SER-11B	HS	-0.07	0.24	4.78
LEU-14B	HS	0.27	0.27	-5.3
<b>SER-15B</b>	HS	0.76	0.37	-0.7
PHE-16B	HS	3.16	1.03	-20.09
<b>PHE-19B</b>	HS	3.40	1.02	-27.66
ALA-20B	HS			-4.92
<b>VAL-21B</b>	HS	1.46	2.08	-17.08
ALA-26B	HS			-3.62
<b>ASP-29B</b>		1.37	1.51	-28.04
TYR-30B				-5.05
<b>SER-33B</b>				0.85
<b>ASN-40B</b>	HS	1.78	0.32	1.56
CYS-41B				-2.5
VAL-42B	HS	1.87	1.98	-18.43
<b>LYS-43B</b>				3
MET-44B		1.21	0.51	-18.26
<b>LEU-45B</b>				-9.55
<b>THR-58B</b>				-3.17
PRO-59B				-2.87
GLY-69B	HS			-3.78
ALA-71B	HS			-7.95
SER-72B	HS	-0.16	0.33	-4.35
ARG-78B	HS	2.54	0.91	10.65
CYS-79B	HS	-0.02	0.15	-0.21
HIS-80B	HS	1.28	0.08	-0.36
ILE-81B				4.22
GLY-88B				1.48
PHE-89B				-9.28
<b>CYS-90B</b>				1.26
<b>LYS-93B</b>	HS	2.28	2.04	61.15
<b>GLY-94B</b>				-2.44
LYS-95B				-8.57
<b>TYR-96B</b>	HS	2.38	2.84	-5.52

\*HS: Hotspot; Predicted HS depicted in red; H-bond forming residues depicted in blue

**Table S33.** List of interacting residues at protein-protein interacting interface of MERS-CoV NSP14 (Chain A) and NSP10 (Chain B), interface hotspot residues are predicted using three computational methods implemented in KFC, DrugScore<sup>PPI</sup> and Robetta web server. The per-residue energy decomposition analysis was carried out using the last 20 ns MD trajectory.

<b>Residues</b>	<b>KFC</b>	<b>Robetta <math>\Delta\Delta G</math> (kcal/mol)</b>	<b>DrugScore PPI <math>\Delta\Delta G</math> (kcal/mol)</b>	<b>Per-residue energy contribution (kJ/mol)</b>
LEU-7A		1.27		-4.56
PHE-8A	HS	2.53		-8.75
PRO-20A	HS			-1.44
<b>ALA-21A</b>	HS			-6.87
TYR-22A		1.07	1.91	-6.21
ALA-23A	HS			-0.22
PRO-24A	HS			-4.72
THR-25A				-2.29
<b>TYR-26A</b>				-3.89
VAL-29A				-1.24
LEU-39A		1.37	1.11	-7.69
<b>CYS-40A</b>	HS	-0.11	0.24	-3.1
ASN-42A				-0.02
PHE-60A				-5.47
<b>LYS-61A</b>				15.15
LEU-62A	HS	1.43	0.89	-5.71
ALA-64A				-0.51
VAL-66A	HS	1.23	0.93	-5.68
PRO-67A				-2.2
TYR-69A		1.92	1.00	-1.77
LEU-72A				-1.27
<b>ASP-126A</b>	HS	0.77	1.22	-5.98
<b>THR-127A</b>				-2.43
GLU-128A				-19.1
<b>TRP-129A</b>				-2.7
<b>ASN-131A</b>	HS	1.88	0.65	-1.17
CYS-199A				0.89
LYS-200A		1.34	0.84	-6.64
<b>ILE-201A</b>	HS	0.85	1.47	-3.82
TYR-217A				-1.3
<b>SER-15B</b>	HS	0.81	0.59	-0.43
LEU-16B	HS	1.01	0.33	-6.99
ASN-18B				-2.9
<b>PHE-19B</b>	HS	3.85	1.20	-14.02
THR-20B	HS	0.82	0.38	-1.39
VAL-21B	HS	1.49	1.67	-9.46
ALA-26B				-0.39
PHE-30B				-4.38
ALA-33B				-1.4

<b>ASN-40B</b>				-3.43
VAL-42B	HS	1.84	1.37	-9.37
<b>LYS-43B</b>				-6.92
MET-44B		1.29	0.50	-8.23
<b>LEU-45B</b>				-5.79
<b>GLY-69B</b>	<b>HS</b>	-		<b>-1.77</b>
ALA-71B	HS			-4.71
SER-72B				-1.55
ARG-78B				11.63
ALA-79B	HS			-1.71
<b>HIS-80B</b>	HS	2.47	0.29	-3.07
ILE-81B				1.65
VAL-89B				-3.5
<b>CYS-90B</b>				0.19
<b>LYS-93B</b>	HS	1.43	1.30	40.99
<b>GLY-94B</b>				-2.77
LYS-95B				8.6
PHE-96B		1.11	0.54	-4.03

---

\*HS: Hotspot; Predicted HS depicted in red; H-bond forming residues depicted in blue

<b>Table of content</b>		<b>Page no.</b>
<b>Figure S1.</b>	Amino acid sequence alignment of NSP14 of SARS-CoV-2, SARS-CoV and MERS-CoV obtained from Clustal Omega server. Conserved residues among all the three coronaviruses are depicted as	S1
<b>Figure S2.</b>	Amino acid sequence alignment of NSP10 SARS-CoV-2, SARS-CoV and MERS-CoV obtained from Clustal Omega server. Conserved residues among all the three coronaviruses are depicted as ‘*’	S2
<b>Figure S3.</b>	Representation of hydrophobicity map of average structure (from last 20 ns) SARS-CoV-2 (A), SARS-CoV (B) and (C) MERS-CoV NSP14-NSP10 PPI complex in three different forms. Yellow colour depiction is for NSP10, Brown colour is NSP14. The nonpolar (orange), polar (blue) and neutral regions are depicted for the NSP14.	S3
<b>Figure S4.</b>	Figure S4. Radius of gyration (Rg) graphs (a) – (c) of NSP14-NSP10 complexes of SARS-CoV-2, SARS-CoV, MERS-CoV ( left side) and SARS-CoV-2 NSP14mutant complexes (right side) along the three sets of 100 ns MD simulation. Triple mutant (in red, in the left plots) is the combination of the three (F233L, P203, L177F) mutations.	S4
<b>Figure S5.</b>	Superimposed average structures (extracted from the last 20 ns MD trajectories of three sets of MD simulation) of SARS-CoV-2 NSP14-NSP10 complex with SARS-CoV and MERS-CoV (a)-(c). On the left side is the NSP14 RMSF plot depicts the C-terminal fluctuating residues encircled in red (from residue 245-268) in replica 1 (a) and 2 (b). The middle square box represents the corresponding fluctuating residue (245-268).	S5
<b>Figure S6.</b>	Superimposed average structures (from last 20 ns) of (a) NSP10 SARS-CoV-2 (light brown), SARS-CoV (cyan) and MERS-CoV (pink) from the three (b)-(d) sets of MD simulation. Left side represents the RMSF of NSP10 from the three sets of MD simulation (b)-(d). In the middle, superimposed NSP10 3D structure of the three viruses is depicted. On the right side in a square box fluctuating N-terminal region has been focused ranging from 113-131, shows a conformational change from coil to beta strand in case of SARS-CoV (cyan) in all the three sets (b)-(d) of MD simulations..	S6
<b>Figure S7.</b>	(a) – (c) On the left side, representation of superimposed SARS-CoV-2 mutant average structures (from last 20 ns) of NSP14-NSP10 from all the three sets of MD simulations. In a square box in the middle, represented the C terminal fluctuation ranging from residue 113-131 in the NSP10 when it is in complex with mutated NSP14. (a) In case of replica 1, NSP10 with NSP14 (P203L) mutant, shows a conformational change from coil to beta strand. (b) In replica 2, NSP10 with NSP14 (Triple) mutant, shows a conformational change from coil to beta strand. (c) In replica 3, in the right side RMSF plot, does not show much fluctuation as compared to replica 1 and 2, therefore there is no conformational changes observed at position 113-131 (in the middle figure in a square box of replica 3).	S7
<b>Figure S8.</b>	Solvent Accessible Surface Area (SASA) graphs of (a)-(c) SARS-CoV-2, SARS-CoV, MERS-CoV (left side) and SARS-CoV-2 NSP14mutant complexes (right side) along the three sets of 100 ns MD simulation..	S8
<b>Figure S9.</b>	Comparison of the electrostatic surface and charge distribution of NSP14 initial (a)-(c) and average structure (extracted from last 20 ns) (e)-(g) of SARS-CoV-2, SARS-CoV and MERS-CoV. Three views are shown for each PPI complexes. NSP10 secondary structure is depicted in yellow and NSP14 presented in multicolor ribbon and electrostatic charge distribution depicting interface region of NSP14 is shown with positive (blue), negative (red) surface.	S9
<b>Figure S10.</b>	Electrostatic surfaces and charge distribution of the NSP14: comparison of the electrostatic surface of the average structure (extracted from last 20 ns) of wild type NSP14 (a) in comparison with different mutant structures (b)-(e). Three views are shown for each PPI complexes. The encircled area (b) in NSP14 (presented in multicolor as ribbon) is the binding interface region for NSP10 (NSP10 is depicted in yellow ribbon, extreme left side).	S10
<b>Figure S11.</b>	Cartoon view of the (a) NSP14-NSP10 complex of SARS-CoV-2, common interacting interface hotspot residues among the three viruses (SARS-CoV-2, SARS-CoV and MERS-Co) represented in spheres. The NSP14 is represented in brown, NSP10 in yellow. Hotspot residues are represented in brown spheres (in NSP14), yellow spheres (in NSP10). The represented structure is the average conformer extracted from last 20 ns MD trajectory.	S11



---

<b>Table S1.</b>	PBC Cubic box information for SARS-CoV-2, SARS-CoV and MERS-CoV	S12
<b>Table S2.</b>	Comparison of interface statistics of the initial NSP14-NSP10 complexes (before MD) of SARS-CoV-2, SARS-CoV and MERS-CoV with the average complex structures extracted from last 20 ns from 100 ns MD trajectory of replica 1. For each complex, interface statistics obtained from PDBsum server.	S13
<b>Table S3.</b>	Comparison of interface statistics of the initial NSP14-NSP10 complexes (before MD) of SARS-CoV-2, SARS-CoV and MERS-CoV with the average complex structures extracted from last 20 ns from 100 ns MD trajectory of replica 2. For each complex, interface statistics obtained from PDBsum server.	S14
<b>Table S4.</b>	Comparison of interface statistics of the initial NSP14-NSP10 complexes (before MD) of SARS-CoV-2, SARS-CoV and MERS-CoV with the average complex structures extracted from last 20 ns from 100 ns MD trajectory of replica 3. For each complex, interface statistics obtained from PDBsum server.	S15
<b>Table S5.</b>	Total number of H-bond involved in the average conformer of SARS-CoV-2 NSP14-NSP10 complex extracted from last 20 ns MD trajectory of replica 1. The interface H-bond results obtained from PDBsum server.	S16
<b>Table S6.</b>	Total number of H-bond involved in the average conformer of SARS-CoV-2 NSP14-NSP10 complex extracted from last 20 ns MD trajectory of replica 2. The interface H-bond results obtained from PDBsum server.	S17
<b>Table S7.</b>	Total number of H-bond involved in the average conformer of SARS-CoV-2 NSP14-NSP10 complex extracted from last 20 ns MD trajectory of replica 3. The interface H-bond results obtained from PDBsum server.	S18
<b>Table S8.</b>	Total number of H-bond involved in the average conformer of SARS-CoV NSP14-NSP10 complex extracted from last 20 ns MD trajectory of replica 1. The interface H-bond results obtained from PDBsum server.	S19
<b>Table S9.</b>	Total number of H-bond involved in the average conformer of SARS-CoV NSP14-NSP10 complex extracted from last 20 ns MD trajectory of replica 2. The interface H-bond results obtained from PDBsum server.	S20
<b>Table S10.</b>	Total number of H-bond involved in the average conformer of SARS-CoV NSP14-NSP10 complex extracted from last 20 ns MD trajectory of replica 3. The interface H-bond results obtained from PDBsum server.	S21
<b>Table S11.</b>	Total number of H-bond involved in the average conformer of MERS-CoV NSP14-NSP10 complex extracted from last 20 ns MD trajectory of replica 1. The interface H-bond results obtained from PDBsum server	S22
<b>Table S12.</b>	Total number of H-bond involved in the average conformer of MERS-CoV NSP14-NSP10 complex extracted from last 20 ns MD trajectory of replica 2. The interface H-bond results obtained from PDBsum server.	S23
<b>Table S13.</b>	Total number of H-bond involved in the average conformer of MERS-CoV NSP14-NSP10 complex extracted from last 20 ns MD trajectory of replica 3. The interface H-bond results obtained from PDBsum server.	S24
<b>Table S14.</b>	Total number of H-bond involved in the average conformer of SARS-CoV-2 NSP14 <sup>L177F</sup> mutant complex extracted from last 20 ns MD trajectory of replica 1. The interface H-bond results obtained from PDBsum server.	S25
<b>Table S15.</b>	Total number of H-bond involved in the average conformer of SARS-CoV-2 NSP14 <sup>L177F</sup> mutant complex extracted from last 20 ns MD trajectory of replica 2. The interface H-bond results obtained from PDBsum server.	S26
<b>Table S16.</b>	Total number of H-bond involved in the average conformer of SARS-CoV-2 NSP14 <sup>L177F</sup> mutant complex extracted from last 20 ns MD trajectory of replica 3. The interface H-bond results obtained from PDBsum server.	S27
<b>Table S17.</b>	Total number of H-bond involved in the average conformer of SARS-CoV-2 NSP14 <sup>P230L</sup> mutant complex extracted from last 20 ns MD trajectory of replica 1. The interface H-bond results obtained from PDBsum server.	S28
<b>Table S18.</b>	Total number of H-bond involved in the average conformer of SARS-CoV-2 NSP14 <sup>P230L</sup> mutant complex extracted from last 20 ns MD trajectory of replica 2. The interface	S29

---

---

	H-bond results obtained from PDBsum server	
<b>Table S19.</b>	Total number of H-bond involved in the average conformer of SARS-CoV-2 NSP14 <sup>P230L</sup> mutant complex extracted from last 20 ns MD trajectory of replica 3. The interface H-bond results obtained from PDBsum server	S30
<b>Table S20.</b>	Total number of H-bond involved in the average conformer of SARS-CoV-2 NSP14 <sup>F233L</sup> mutant complex extracted from last 20 ns MD trajectory of replica 1. The interface H-bond results obtained from PDBsum server.	S31
<b>Table S21</b>	Total number of H-bond involved in the average conformer of SARS-CoV-2 NSP14 <sup>F233L</sup> mutant complex extracted from last 20 ns MD trajectory of replica 2. The interface H-bond results obtained from PDBsum server.	S32
<b>Table S22</b>	Total number of H-bond involved in the average conformer of SARS-CoV-2 NSP14 <sup>F233L</sup> mutant complex extracted from last 20 ns MD trajectory of replica 3. The interface H-bond results obtained from PDBsum server.	S33
<b>Table S23.</b>	Total number of H-bond involved in the average conformer of SARS-CoV-2 NSP14 <sup>Triple</sup> mutant complex extracted from last 20 ns MD trajectory of replica 1. The interface H-bond results obtained from PDBsum server.	S34
<b>Table S24.</b>	Total number of H-bond involved in the average conformer of SARS-CoV-2 NSP14 <sup>Triple</sup> mutant complex extracted from last 20 ns MD trajectory of replica 2. The interface H-bond results obtained from PDBsum server.	S35
<b>Table S25.</b>	Total number of H-bond involved in the average conformer of SARS-CoV-2 NSP14 <sup>Triple</sup> mutant complex extracted from last 20 ns MD trajectory of replica 3. The interface H-bond results obtained from PDBsum server.	S36
<b>Table S26.</b>	Total number of H-bond involved in the initial structure (before MD) of SARS-CoV-2 NSP14-NSP10 PPI complex interface obtained from PDBsum server	S37
<b>Table S27.</b>	Total number of H-bond involved in the initial structure (before MD) of SARS-CoV NSP14-NSP10 PPI complex interface obtained from PDBsum server	S38
<b>Table S28</b>	Total number of H-bond involved in the initial structure (before MD) of MERS-CoV NSP14-NSP10 PPI complex interface obtained from PDBsum server	S39
<b>Table S29</b>	Salt bridge involved in the initial structure (before MD) of SARS-CoV-2, SARS-CoV and MERS-CoV of NSP14-NSP10 PPI complex. The salt bridges atom-atom interaction at PPI interface obtained from PDBsum server	S40
<b>Table S30</b>	Salt bridge involved in the average conformer of SARS-CoV-2, SARS-CoV and MERS-CoV NSP14-NSP10 complex extracted from last 20 ns MD trajectory from all the three sets of MD simulations. The salt bridge atom-atom interactions across protein-protein interface results are obtained from PDBsum server. In SARS-CoV-2 MD simulation replica 2 and 3, and SARS-CoV-2 <sup>F233L</sup> replica 2 does not form salt bridges.	S41
<b>Table S31</b>	List of interacting residues at protein-protein interacting interface of SARS-CoV-2 NSP14 (Chain A) and NSP (Chain B), interface hotspot residues are predicted using three computational methods implemented in KFC, DrugScore <sup>PPI</sup> and Robetta web server. The per-residue energy decomposition analysis was carried out using the last 20 ns MD trajectory.	S42-43
<b>Table S32</b>	List of interacting residues at protein-protein interacting interface of SARS-CoV NSP14 (chain A) and NSP10 (chain B), interface hotspot residues are predicted using three computational methods implemented in KFC, DrugScore <sup>PPI</sup> and Robetta web server. The per-residue energy decomposition analysis was carried out using the last 20 ns MD trajectory.	S44-45
<b>Table S33</b>	List of interacting residues at protein-protein interacting interface of MERS-CoV NSP14 (chain A) and NSP8 (chain B), interface hotspot residues are predicted using three computational methods implemented in KFC, DrugScore <sup>PPI</sup> and Robetta web server. The per-residue energy decomposition analysis was carried out using the last 20 ns MD trajectory.	S46-47

---

